SolarPACES 2024, 30th International Conference on Concentrating Solar Power, Thermal, and Chemical Energy Systems

Analysis and Simulation of CSP and Hybridized Systems

https://doi.org/10.52825/solarpaces.v3i.2275

© Authors. This work is licensed under a Creative Commons Attribution 4.0 International License

Published: 19 Nov. 2025

# Linear Fresnel Ray Tracing Analysis: Southern Italy Plant Optimization Through FresnelSim Algorithm

An Analysis of the Main Design Parameters of the Primary Concentrator and an Insight on Compound Parabolic Collector Effectiveness



<sup>1</sup>Department of Mechanical, Energy, Management and Transportation Engineering, University of Genova, Italy \*Correspondence: Samuele Memme, samuele.memme@edu.uniqe.it

Abstract. The goal of maximizing the optical efficiency of a Linear Fresnel Collector is typically addressed through Monte Carlo Ray Tracing simulations. This study introduces FresnelSim, a 3D ray tracing software developed at the University of Genoa, Italy, for the optical analysis of Linear Fresnel Collectors. FresnelSim has been herein used to examine key geometric factors and their impact on a reference plant's producibility, allowing to almost triple the irradiance at the secondary concentrator with respect to a reference base configuration. Through a series of fast parametric simulations, an optimized geometry for such a system is proposed, highlighting to which extent different efficiency indicators are dependent on mirrors' gap, field length and mirrors' radius of curvature. Then, an assessment of the effect of the plant's azimuthal orientation in the range from 0° to 45° is presented, showing that the site's yearly average producibility is reduced up to 3.3% as an effect of primary mirror alignment. Finally, an analysis of the Compound Parabolic Collector is presented in terms of sub hourly opto-energy efficiency for 3 reference days, resulting in values ranging from 80.9% to 87.4%. Energy flux circumferential uniformity at the absorber tube is evaluated under 6 different incidence angles, highlighting that irradiance uniformity could be further enhanced by a properly defined mirrors' motion law.

**Keywords:** Linear Fresnel Collector Optimization, Raytracing, Irradiance Uniformity, Collector Orientation

## 1. Nomenclature

Greek letters	
αs	Solar altitude angle [°]
β	Tilt angle of primary mirrors [°]
γs	Solar azimuth angle [°]
δ	Declination solar angle [°]
ζ	Primary mirror orientation [°]
η	Opto-energy efficiency
$\theta_{a}$	Acceptance angle of the CPC reflector [°]
$\theta_{w}$	Incidence angle [°]
μ	Average
σ	Standard deviation
φ	Latitude [°]
ω	Angular coordinate of the absorber tube [°]
Acronyms	
CPC	Compound parabolic collector
CSP	Concentrating solar power
DNI	Direct normal irradiance
LFC	Linear Fresnel collector
MCRT	MonteCarlo ray tracing
UI	Uniformity index
Symbols	
Apcec	Secondary receiver aperture width [m]
$E_{r,j,i}$	Share of solar irradiance of the single j <sup>th</sup> ray on the i <sup>th</sup> mirror [Wh/m²]
g	Gap, horizontal spacing between adjacent mirrors [m]
L <sub>m</sub>	Length of the primary mirror row [m]
$\vec{N}$	Normal vector to mirror's surface
N <sub>day</sub>	Day number
Ř	Vector representing reflected ray direction
r <sub>1</sub> , r <sub>2</sub>	Internal and external radius of the absorber tube [m]
Ŝ	Vector pointing sun position
t <sub>0</sub>	Height of the absorber tube with respect to CPC aperture [m]
W <sub>m</sub>	Width of the single primary mirror [m]
X <sub>m,i</sub>	Distance of the i <sup>th</sup> mirror axis from the LFC axis of symmetry [m]

### 2. Introduction

The analysis and optimization of geometric parameters in Linear Fresnel Collector (LFC) systems to maximize their energy output is a critical area of interest in the modeling of Concentrating Solar Power (CSP) systems. LFC optical performance is influenced by factors such as shading and blocking effects by neighbour mirrors, primary mirror alignment and curvature, solar incidence angle, end-effects, tracking, and manufacturing errors, as well as the shape and efficiency of the secondary receiver. In the literature, several studies have aimed to identify the best design and operational conditions according to different criteria, focusing on primary mirrors' geometry and arrangement, field orientation, and characteristics of the energy flux at the secondary receiver.

The effect of mirror focal distance on a reference plant has been assessed by Shaoxuan et al. [1] through MCRT (Monte Carlo ray tracing)-validated analytical equations and by Boito and Grena [2]; similarly, Heimsath et al. [3] tackled the end-losses issue by proposing the substitution of the actual receiver height with an effective one. The influence of mirrors spacing has been studied by many authors: among them, Abbas et al. [4] compared the variable gap

with the variable width strategy, while in [5] by Singh et al. the optical efficiency of a LFC has been assessed by varying both the number of mirrors and the gap between them. Mathur et al. [6] proposed a method to minimize shading and blocking at solar noon; Boito and Grena [7] developed a specific cost function to determine the optimal plant geometry. Bellos et al. [8] conducted an experimental and numerical investigation of a linear Fresnel collector with a flat plate receiver located in Athens, Greece. Barbòn et al. [9] analyzed the effects of the number, width and position of the primary mirrors and the height, length and relative position of the single absorber tube, whereas Gonzalez-Mora et al. [10] proposed an optimization of the FRESDEMO Fresnel field to find the best receiver height and secondary reflector geometry.

Another variable that can affect the amount of collectible energy from a generic solar system is the orientation of the plant, i.e. the azimuth angle of the longitudinal axis of the system with respect to the north-south direction: it is known that east-west orientations can provide less variable energy outputs, while north-south ones lead to the highest daily energy collection peaks [11]. Some published works considered the effect of LFC orientation on its optical efficiency: Huang et al. [12] proposed an LFC equipped with a solar azimuth tracking system validated by MCRT, whereas an analytical approach has been proposed by Sharma et al. [13]. Montanet et al. have studied a real facility [14] in the frame of a comprehensive analysis of a plant located in France.

The LFC geometry can influence not only the amount of energy collection but also the irradiation distribution on the absorber tube. Chaitanya Prasad et al. [15] introduced an optimization method for mirror tilt and radii to achieve uniform flux distribution over the absorber tube. The analysis by Benyakhlef et al. [16] was instead specifically devoted to the determination of the best mirrors' radius of curvature for a homogeneous flux density distribution and best optical efficiency of the system. Pulido-Iparraguirre et al. [17] proposed a novel arrangement of a cylindrical-mirror LFC aimed at having a homogeneous thermal power profile delivered along the year.

In this paper, a ray-tracing algorithm named FresnelSim is employed to analyze the impact of various geometric design parameters on the performance of an LFC. Starting from a known geometry based on a real facility, different design parameters are parametrically modified to determine an optimal configuration. This process utilizes the functionalities of the simulation code specifically developed for such systems by the present Authors, capable of providing a range of optical and energy efficiency indicators. Subsequently, the effect of a non-optimal collector orientation, which is commonly assumed to be aligned along the north-south axis in most analyses, is evaluated with reference to the system's final geometry. Lastly, the performance of the secondary concentrator (CPC type) is assessed over a series of typical days, highlighting its average value and daily variability. The irradiance at the receiver tube is then evaluated in terms of radial uniformity, demonstrating its dependence on the angle of incidence and suggesting the use of improved primary mirror motion laws able to minimize the radial variability of the energy flux.

# 3. Modelling

FresnelSim model, whose working principle and validation against Tonatiuh software [18] have been extensively presented in [19], is a simulation tool based on MCRT approach especially devoted to optical and energy calculations on LFC. The algorithm has been developed in MATLAB environment and is conceived to assess different optical and energy efficiencies of a LFC equipped either with flat or cylindrical primary mirrors and a CPC secondary collector.

# 3.1 A 3D raytracing model for LFC

FresnelSim introduces several innovative features tailored for the study of linear Fresnel systems, simplifying the modification of geometric parameters for both the primary mirror field and the secondary receiver.

These parameters include primary mirror length  $(L_m)$ , width  $(W_m)$ , radius of curvature  $(R_m)$ , spacing (g), receiver height  $(H_t)$ , and the geometric characteristics of the Compound Parabolic Concentrator (CPC), in particular aperture width of the cavity  $(Ap_{CPC})$ , acceptance angle  $(\theta_a)$ , position of the absorber tube  $(t_0)$ , inner and outer radius of the evacuated tube  $(r_1$  and  $r_2)$ . Additionally, it encompasses optical parameters such as mirror reflectivity, receiver tube absorptivity, tracking system errors, and angular deviations of reflected rays.

FresnelSim allows for simulations over various time horizons, i.e. instantaneous, daily, or annual averages, providing a comprehensive analysis of how design parameters affect energy availability and optical-energy efficiency through time. The software evaluates the plant efficiency considering energy directed to the CPC aperture or to the vacuum tube, and it can separately assess individual optical losses, such as shading, blocking, end losses, and cosine efficiency. Moreover, the sun position can be described by taking in consideration the orientation of the LFC ( $\zeta$ ) as measured with respect to the north-south direction, according to Eq. (1), expressed as function of solar altitude ( $\alpha_s$ ) and azimuth angles ( $\gamma_s$ ).

$$\vec{S} = [S_x, S_y, S_z] = [\cos(\alpha_s) \cdot \cos(\gamma_s - \zeta), \cos(\alpha_s) \cdot \sin(\gamma_s - \zeta), \sin(\alpha_s)]$$
 (1)

According to Snell's reflection law,  $\vec{R}_i$  is the vector representing the reflected ray by the i<sup>th</sup> mirror, being the tilt angles  $\beta_i$  of the i<sup>th</sup> mirror calculated to direct it to the axis of symmetry of the CPC. To calculate the reflected ray, the normal vector to each mirror  $\vec{N}_i$  is required, as shown in Eq. (2).

$$\vec{R}_i = \vec{S} - 2 \cdot (\vec{S} \cdot \vec{N}_i) \cdot \vec{N}_i \tag{2}$$

In turn,  $\vec{N_i}$  is dependent on the mirrors' tilt, that is calculated according to the following Eq. (3), where  $x_{m,i}$  represents the distance of the i<sup>th</sup> mirror axis of rotation from the LFC axis of symmetry.

$$\beta_i = \tan^{-1} \left( \frac{\frac{x_{m,i}}{R} - S_x}{\frac{H_t}{R} - S_z} \right) \tag{3}$$

The complete set of governing equations is reported in papers [11,19-20]. These encompass the description of shading, blocking, angular deviation of the tracking system, angular deviation of the reflected rays due to non-perfect reflection, multiple reflections within the CPC and a full set of performance estimates.

One of the required inputs is the number of rays to be initialized on each mirror i ( $N_{rays,i}$ ): a given amount of energy [Wh] has to be associated with each initialized ray ( $E_{r,j,i}$ ). This quantity is calculated as a function of the hourly-averaged direct normal irradiance DNI [W/m²], of the single mirror area and of the well-known "cosine efficiency", i.e. the cosine of the angle of incidence on the  $i^{th}$  mirror ( $\theta_{w,i}$ ).  $E_{r,j,i}$  is finally calculated as in the following Eq. (4).

$$E_{r,j,i} = \frac{DNI \cdot L_m \cdot W_m \cdot \cos(\theta_{w,i})}{N_{rays}} \tag{4}$$

For the aim of this study, two efficiency indicators are used:  $\eta_1$ , expressed by Eq. (5), represents the solar energy flux at the CPC aperture plane over the insolation on an area equal to the total mirrors' surface, while  $\eta_2$ , Eq. (6), is referred to the gross area occupied by the LFC.

$$\eta_{1} = \frac{\sum_{i=1}^{N_{mir}} \sum_{j=1}^{N_{rays,i}} E_{r,j,i}}{DNI \cdot W_{m} \cdot L_{m} \cdot N_{m}}$$
 (5)

$$\eta_{2} = \frac{\sum_{i=1}^{N_{mir}} \sum_{j=1}^{N_{rays,i}} E_{r,j,i}}{DNI \cdot [L_{m} \cdot N_{mir} \cdot (W_{m} + g) - g \cdot L_{m}]}$$
(6)

A further indicator, specifically used for estimating irradiation uniformity on the absorber tube, is provided in Eq. (7), where  $\sigma_{\omega}$  is the standard deviation of the solar energy flux with respect to the angular coordinate  $\omega$  and  $\mu$  is the average over the entire tube surface. U.I. is comprised by definition in the range between 0 and 1.

$$U.I. = 1 - \frac{\sigma_{\omega}}{\mu} \tag{7}$$

#### 3.2 FresnelSim validation

The proposed ray tracing algorithm has been carefully validated against reliable data: in detail, a series of sub-hourly simulations has been carried out by means of Tonatiuh MCRT code. In this case, the 16 considered mirrors are flat and they are aligned along the north-south direction: the Tonatiuh results are compared to FresnelSim predictions. For the sake of brevity, the results are presented for some reference days, namely the solstices and equinoxes (i.e. days number 81, 172, 355). Ray tracing runs are performed at a time step equal to 30 minutes, with some  $10^6$  initialized rays at each simulation: a convergence analysis based on the generated ray number applied to Tonatiuh simulations shows that the selected value is reliable for obtaining the expected accuracy in convergence. The root mean square error (RMSE) between the values obtained from Tonatiuh and FresnelSim was found to be as low as 0.26% during the winter solstice, 1.41% during the summer solstice and 0.72% at the equinoxes. Furthermore, not only do the daily trends exhibit substantial overlap, but also nearly all instantaneous efficiency values show an error of less than 5.0% when compared to the "exact" Tonatiuh ones, with a coefficient of determination ( $r^2$ ) equal to 0.999 (Figure 1).

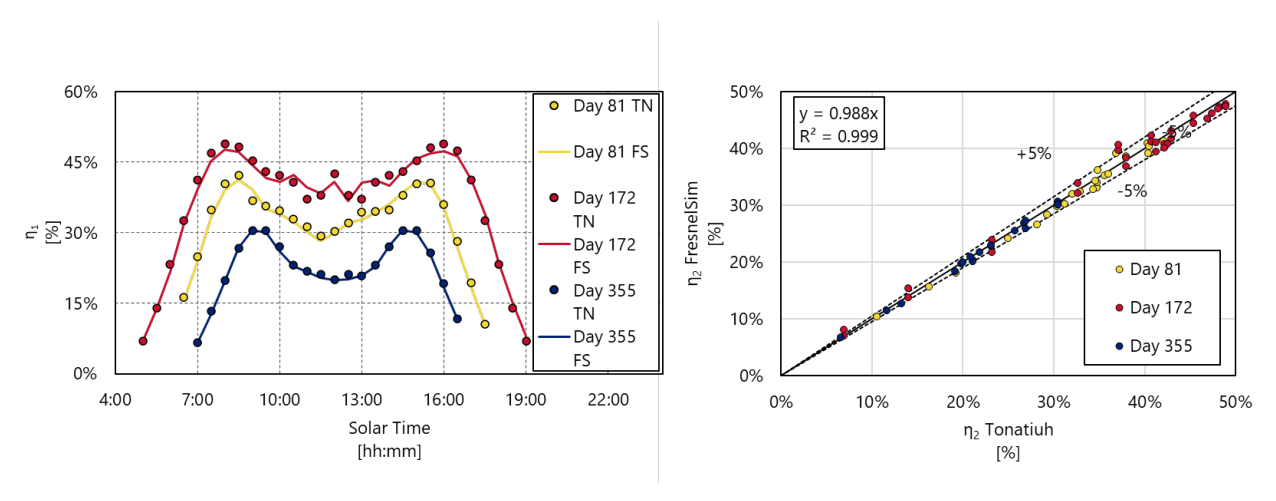


Figure 1. Daily efficiency trends: comparison between Tonatiuh (TN) and FresnelSim (FS) results

# 3.2 The case study: Partanna LFC, Italy

The analysis presented in this study refers to the geometry of a plant operating in Partanna, Italy, with design data obtained from publicly available online sources or approximate measurements taken from satellite images. Specifically, the *base* configuration consists of a single module with 16 primary mirrors with length of 57 m, a width equal to 0.8 m, and gaps between adjacent mirrors of 0.3 m (Figure 2). The height of the secondary receiver's aperture plane is 7.5 m above the plane of primary mirrors level, thus resulting in an aspect ratio (AR), here

defined as the ratio of mirrors' length to receiver height, equal to 7.6. The mirrors, whose radius of curvature is unknown, are assumed to be flat in the *base* (reference) configuration of the plant.

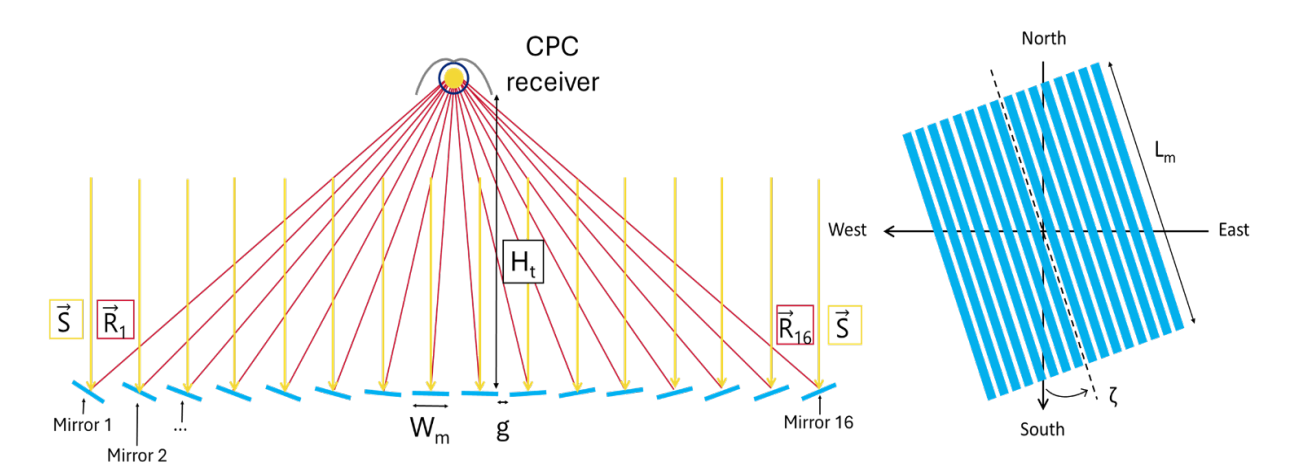


Figure 2. Schematic representation of the Partanna plant: primary field dimensions and orientation.

The geometry of the CPC collector was derived from measurements conducted by the authors and reported in [20]. Specifically, the geometric description of the secondary concentrator requires knowledge of the inner  $(r_1)$  and outer  $(r_2)$  radii of the evacuated tube housed within the CPC: in this analysis, their values are set equal to 0.035 m and 0.062 m, respectively. Additionally, the acceptance angle  $(\theta_a)$ , defined as the maximum angle at which sunlight can be captured by the truncated CPC, was determined through trial and error based on measured data and has been estimated equal to 44.5°. Input data for  $\theta_a$  include the aperture width of the concentrator  $Ap_{CPC}$  (0.318 m) and the distance of the truncation line from the axis of the evacuated tube  $t_0$  (0.065 m). In Figure 3, the angular coordinate  $\Gamma$  represents the reference used for subsequent calculations of uniformity along the receiver tube (Chapter 3.3).

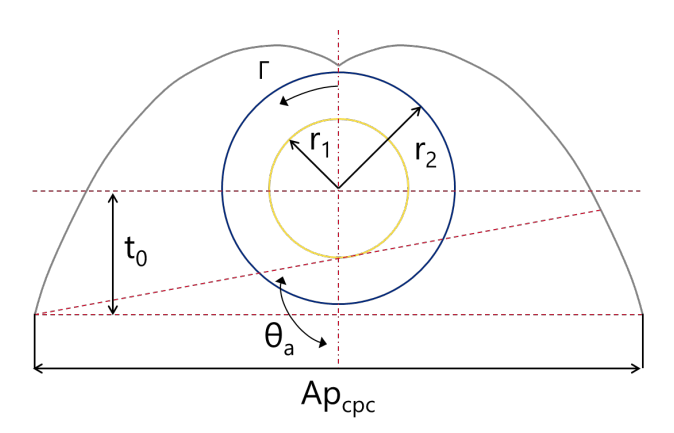


Figure 3. Section representing the CPC receiver geometry and the evacuated tube.

The collector's full set of dimensions, properties and orientation is reported in [20].

### 4. Results

The parametric analysis of the north-south aligned plant proceeded in several steps (whereas the real plant is oriented approximately 26° NW, the present analysis started from the north-south configuration). Firstly, the real performance of the plant has been evaluated through the analysis of the opto-energy efficiency index: its value, considering year-long daily averages, is equal to 19.9% according to Eq. (3), 14.7% if calculated with respect to the gross field area.

The above low efficiency values, in the reference configuration, have to be ascribed to the high number of lost rays at the secondary mirror, due to the non correct focusing of them by the flat primary mirrors.

## 4.1 Optimization of plant geometry

The first parameter taken in consideration to investigate its effect on the final efficiency of the plant is the gap between adjacent mirrors, which is herein assumed to be constant for each mirrors' row. In this step, it is particularly evident that defining an appropriate efficiency index is necessary to evaluate the actual beneficial effect of a modification in the plant's geometry, in this case by reducing from 0.3 m to 0.1 m the mirrors' gap. Specifically, when considering the efficiency  $\eta_1$ , it slightly decreases to 19.0% due to the increased influence of shading and blocking effects caused by the closer proximity of the mirrors. Conversely, when considering the efficiency  $\eta_2$ , which refers to the entire area occupied by the reflectors, it amounts to 17%, with an average annual increase of 2.3% compared to the <code>base</code> case. To resolve this apparent dichotomy, one can directly consider the energy available at the receiver aperture, which notably increases by 18.2%. This is due to the fact that a smaller gap leads to higher cosine efficiencies and increased land-use during peak DNI hours, while the effect of increased shading and blocking has a minor effect, being mainly related to early morning or late afternoon hours.

The second parameter analyzed is the aspect ratio (AR). Specifically, the analysis aims to determine the module length required to render end-losses negligible on an annual basis. Consequently, the AR has been considered as a function of mirror length only, with the receiver height (H<sub>t</sub>) kept constant at 7.5 m. Yearly simulations concluded that end-losses can be effectively reduced up to AR as high as 20, above which no significant performance improvement can be observed: this further improved configuration results in an additional 5% increase in the available energy and a yearly average efficiency  $\eta_1$  equal to 20.0% ( $\eta_2$  = 18.0%). Daily peaks occur during summer, reaching maximum average values equal to 24.0% (21.5%); considering the ratio of daily values standard deviation and yearly average energy flux at the receiver, the reduction of end-losses lead also to a 10% reduction in the day-by-day variability.

Finally, the focus has been shifted towards the calculation of the optimal primary mirrors' radius of curvature ( $R_m$ ), assuming a constant value for all the mirrors' rows. To make the analysis non-dimensional, multiple values of the receiver height has been considered to identify the best  $R_m$  value. As shown in Figure 4 (left), a radius of curvature equal to 3 times  $H_t$ , i.e. approximately 22.5 m, has been identified as the one able to maximize annual efficiency. According to this improved geometry, the yearly average value of daily efficiencies  $\eta_1$  is equal to 47.8% ( $\eta_2$  = 42.8%): with respect to the starting *base* configuration, this improved one can provide at the receiver almost 3 times as much energy per land unit area, thus highlighting that the radius of curvature has the greatest influence in maximizing energy yield among the considered geometric parameters. The highest daily average values of the two efficiencies calculated at the aperture plane of the CPC receiver equal, respectively, 57.6% and 51.5%; more in detail, the sub-hourly trend of these values are represented in Figure 4 (right), which shows the instantaneous efficiencies, ranging from 0 to 84.5% (76.3%).

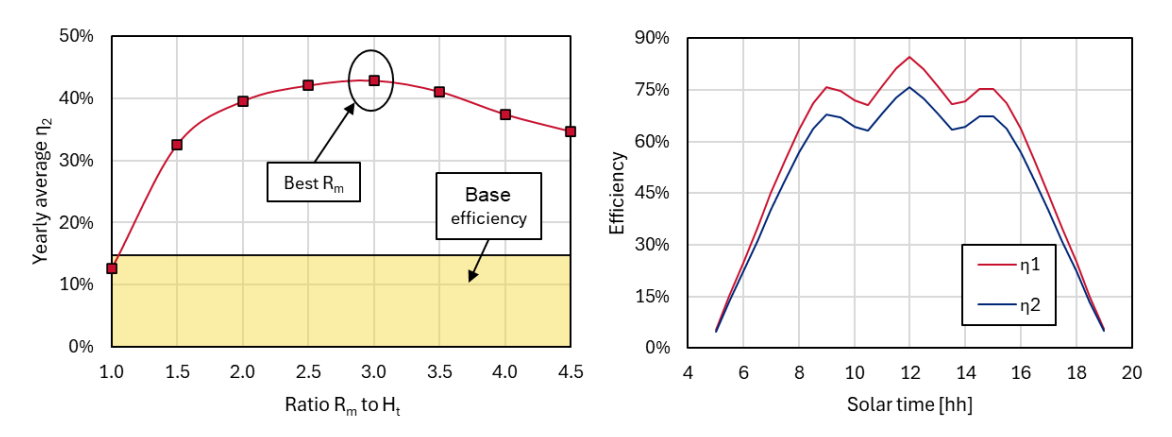


**Figure 4.** Yearly average efficiency as a function of mirrors' radius of curvature (left) and daily trend of instantaneous efficiencies during day 196 (right)

# 4.2 Effect of LFC orientation of primary mirrors

Finally, a parameter that typically affects the performance of real plants is the orientation of the LFC: though north-south orientation is usually assumed during such analyses, operating plants could be aligned along different directions due to geographical constraints and topology of the area. Here, a short overview of how this influences the performance of the final optimized LFC module is provided: with a step of  $15^{\circ}$ , orientations up to  $45^{\circ}$  due to east (or west) have been considered, resulting in a maximum reduction of the daily average value of irradiance collected at the receiver aperture up to 3.3% for orientations equal to  $\mp 45^{\circ}$ . The efficiency daily profile, which is expected to be almost symmetrical for north-south oriented plants, assumes different shapes for other alignments: this could be of particular interest for those applications where weather conditions usually differ from morning to afternoon, thus potentially magnifying the effect of a non-optimal orientation.

# 4.3 Analysis of flux distribution on the CPC tube

This section provides a focus on the results obtained from analyzing the performance of the CPC concentrator. An interesting indicator of the opto-energetic efficiency of the secondary receiver is given by the ratio between the solar flux density at the absorber tube and the irradiation at the aperture plane: as a simple indicator of the CPC effectiveness, this parameter, which is represented in the left side of Figure 5 for three reference days, expresses the share of solar flux entering the secondary concentrator able to transfer heat to the working fluid flowing inside the evacuated tube. The algorithm considers the combined effect of CPC reflector's reflectivity and tube's transmissivity when multiple reflections occur. As shown, instantaneous values range from 80.9% to 87.4%, with almost constant daily averages of 84.5% throughout the year.

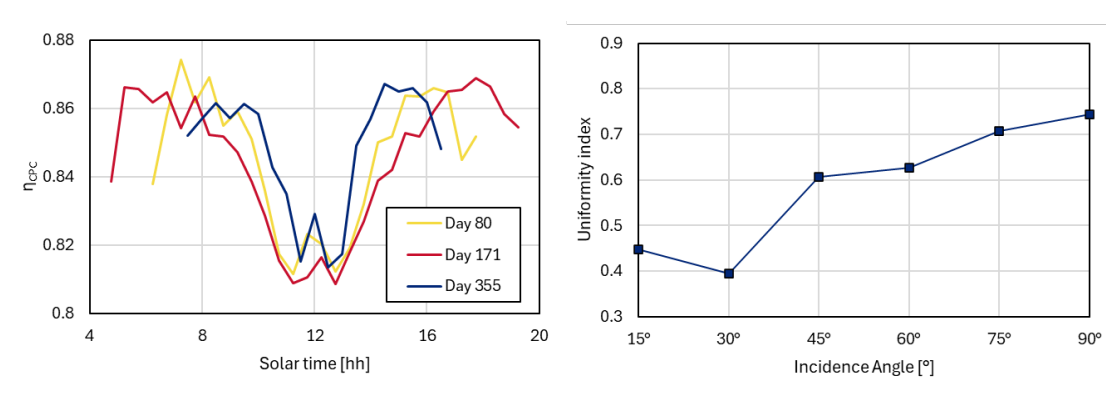


**Figure 5.** Ratio of solar energy flux at the absorber tube and at the CPC aperture plane for three reference days

For a more in-depth analysis, the uniformity index (U.I.) as defined in Eq. 5 was considered, with the tube divided into sectors identified by an angle of  $4^{\circ}$ , resulting in a total of 90 circumferential regions (Figure 6). The cylinder was further subdivided in 4 longitudinal parts, but the flux does not show significative variations along this direction, so the calculation of the U.I. has been performed just as a function of the  $\omega$  angular coordinate.

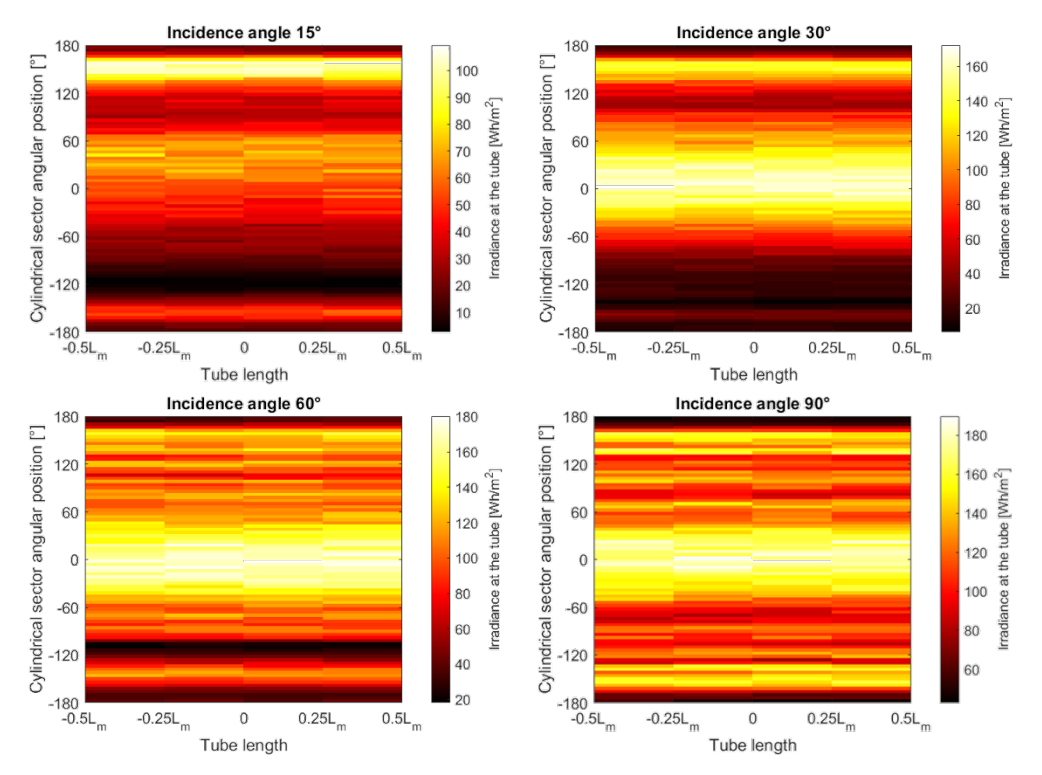


Figure 6. Solar irradiance distribution on the receiver evacuated tube at different incidence angles

The analysis presented here is based not only on the simulation of typical days but also on the parametric variation of the sun's incidence angle, with the solar azimuth set to 90° (east) and the solar altitude varying between 10° and 90°. As shown in Figure 5 (right), U.I. increases up to 0.74, obtained for an incidence angle of 90°. Since it is possible to define uniformity indicators using different formulas, comparing values from different analyses is not always straightforward: however, the aim of this analysis is to highlight how the current mirror motion law, which targets the center of the secondary receiver, might not be the best if the goal is to achieve a more uniform flux at the receiver tube.

### 5. Conclusions

In this paper, the *base* configuration of a Linear Fresnel Collector (LFC) utilizing flat mirrors was analyzed and further optimized to reach maximum opto-energy efficiency values. Using a specially developed 3D ray tracing software, named FresnelSim, an improved geometry of the primary reflectors was proposed. Specifically, the gap between the mirrors was optimized to achieve higher cosine efficiency during hours of maximum Direct Normal Insolation (DNI), highlighting that minimal gaps should be preferred. Additionally, the field length was determined with respect to receiver height to minimize end-losses; then an optimal radius of curvature for the primary mirrors was calculated, resulting in an average annual concentrated irradiation increase at the CPC by three times compared to the *base* configuration. The effect of the plant's orientation was also considered, showing a 3.3% reduction in its productivity when deviating 45° from the north-south alignment. Finally, the performance of the CPC receiver was analyzed over three typical days, revealing efficiencies between 80% and 88%. The energy flux distribution at the receiver tube was evaluated using a specifically defined indicator, showing increasing values for incidence angles from 30° to 90°.

# Data availability statement

The paper is not based on data.

## **Author contributions**

Conceptualization: S.M., Data curation: S.M., Formal Analysis: S.M.&M.F., Funding acquisition: n.a., Investigation: S.M.&M.F., Methodology: S.M.&M.F., Project administration: n.a., Resources: M.F., Software: S.M., Supervision: M.F., Validation: S.M.&M.F., Visualization: S.M., Writing – original draft: S.M.&M.F., Writing – review&editing: n.a.

# Competing interests

The authors declare that they have no competing interests.

# Acknowledgement

ENEA research centre, Solar Thermal Division, is acknowledged for the useful discussions provided about the Partanna Fresnel Plant. The Authors also acknowledge Dr. Alessia Boccalatte for her contributions to developing parts of the FresnelSim code.

### References

- [1] P. Shaoxuan, X. Chaofeng, End-Effect of Linear Fresnel Collectors, in: 2011 Asia-Pacific Power and Energy Engineering Conference, IEEE, 2011: pp. 1–4. <a href="https://doi.org/10.1109/APPEEC.2011.5748793">https://doi.org/10.1109/APPEEC.2011.5748793</a>.
- [2] P. Boito, R. Grena, Optimal focal length of primary mirrors in Fresnel linear collectors, Solar Energy 155 (2017) 1313–1318. <a href="https://doi.org/10.1016/j.solener.2017.07.079">https://doi.org/10.1016/j.solener.2017.07.079</a>.
- [3] A. Heimsath, G. Bern, D. van Rooyen, P. Nitz, Quantifying Optical Loss Factors of Small Linear Concentrating Collectors for Process Heat Application, Energy Procedia 48 (2014) 77–86. <a href="https://doi.org/10.1016/j.egypro.2014.02.010">https://doi.org/10.1016/j.egypro.2014.02.010</a>.
- [4] R. Abbas, J.M. Martínez-Val, Analytic optical design of linear Fresnel collectors with variable widths and shifts of mirrors, Renew Energy 75 (2015) 81–92. https://doi.org/10.1016/J.RENENE.2014.09.029.
- [5] P.L. Singh, S. Ganesan, G.C. Yàdav, Performance study of a linear Fresnel concentrating solar device, Renew Energy 18 (1999) 409–416. <a href="https://doi.org/10.1016/S0960-1481(98)00805-2">https://doi.org/10.1016/S0960-1481(98)00805-2</a>.
- [6] S.S. Mathur, T.C. Kandpal, B.S. Negi, Optical design and concentration characteristics of linear Fresnel reflector solar concentrators—II. Mirror elements of equal width, Energy Convers Manag 31 (1991) 221–232. https://doi.org/10.1016/0196-8904(91)90076-U.
- [7] P. Boito, R. Grena, Optimization of the geometry of Fresnel linear collectors, Solar Energy 135 (2016) 479–486. https://doi.org/10.1016/j.solener.2016.05.060.
- [8] E. Bellos, D. Korres, C. Tzivanidis, K.A. Antonopoulos, Design, simulation and optimization of a compound parabolic collector, Sustainable Energy Technologies and Assessments 16 (2016) 53–63. <a href="https://doi.org/10.1016/j.seta.2016.04.005">https://doi.org/10.1016/j.seta.2016.04.005</a>.
- [9] A. Barbón, N. Barbón, L. Bayón, J.A. Otero, Theoretical elements for the design of a small scale Linear Fresnel Reflector: Frontal and lateral views, Solar Energy 132 (2016) 188–202. https://doi.org/10.1016/j.solener.2016.02.054.
- [10] E. González-Mora, Ma.D. Durán García, Methodology for an Opto-Geometric Optimization of a Linear Fresnel Reflector for Direct Steam Generation, Energies (Basel) 13 (2020) 355. <a href="https://doi.org/10.3390/en13020355">https://doi.org/10.3390/en13020355</a>.

- [11] S. Memme, M. Fossa, Ray tracing analysis of linear Fresnel concentrators and the effect of plant azimuth on their optical efficiency, Renew Energy 216 (2023) 119121. https://doi.org/10.1016/j.renene.2023.119121.
- [12] F. Huang, L. Li, W. Huang, Optical performance of an azimuth tracking linear Fresnel solar concentrator, Solar Energy 108 (2014) 1–12. https://doi.org/10.1016/j.solener.2014.06.028.
- [13] V. Sharma, J.K. Nayak, S.B. Kedare, Effects of shading and blocking in linear Fresnel reflector field, Solar Energy 113 (2015) 114–138. https://doi.org/10.1016/j.solener.2014.12.026.
- [14] E. Montanet, S. Rodat, Q. Falcoz, F. Roget, Influence of topography on the optical performances of a Fresnel linear asymmetrical concentrator array: The case of the eLLO solar power plant, Energy 274 (2023) 127310. <a href="https://doi.org/10.1016/j.energy.2023.127310">https://doi.org/10.1016/j.energy.2023.127310</a>.
- [15] G.S. Chaitanya Prasad, K.S. Reddy, T. Sundararajan, Optimization of solar linear Fresnel reflector system with secondary concentrator for uniform flux distribution over absorber tube, Solar Energy 150 (2017) 1–12. <a href="https://doi.org/10.1016/j.solener.2017.04.026">https://doi.org/10.1016/j.solener.2017.04.026</a>.
- [16] S. Benyakhlef, A. Al Mers, O. Merroun, A. Bouatem, N. Boutammachte, S. El Alj, H. Ajdad, Z. Erregueragui, E. Zemmouri, Impact of heliostat curvature on optical performance of Linear Fresnel solar concentrators, Renew Energy 89 (2016) 463–474. https://doi.org/10.1016/j.renene.2015.12.018.
- [17] D. Pulido-Iparraguirre, L. Valenzuela, J.-J. Serrano-Aguilera, A. Fernández-García, Optimized design of a Linear Fresnel reflector for solar process heat applications, Renew Energy 131 (2019) 1089–1106. <a href="https://doi.org/10.1016/j.renene.2018.08.018">https://doi.org/10.1016/j.renene.2018.08.018</a>.
- [18] M.J. Blanco, J.M. Amieva, A. Mancillas, The Tonatiuh Software Development Project: An open source approach to the simulation of solar concentrating systems, in: ASME 2005 International Mechanical Engineering Congress and Exposition, American Society of Mechanical Engineers, 2005: pp. 157–164.
- [19] M. Fossa, A. Boccalatte, S. Memme, Solar Fresnel modelling, geometry enhancement and 3D ray tracing analysis devoted to different energy efficiency definitions and applied to a real facili-ty, Solar Energy 216 (2021) 75–89. https://doi.org/10.1016/j.solener.2020.12.047.
- [20] S. Memme, M. Fossa, A novel approach for incidence angle modifier calculation of arbitrarily oriented linear Fresnel collectors: Theory, simulations and case studies, Renew Energy 222 (2024) 119857. <a href="https://doi.org/10.1016/j.renene.2023.119857">https://doi.org/10.1016/j.renene.2023.119857</a>.